Drug and Alcohol Dependence 197 (2019) 315–325

Contents lists available at ScienceDirect

Drug and Alcohol Dependence

journal homepage: www.elsevier.com/locate/drugalcdep

Full length article

Influence of experimental alcoholism on the repair process of bone defects filled with beta-tricalcium phosphate

Karina Torres Pomini[a], Tânia Mary Cestari[a], Íris Jasmin Santos German[b], Marcelie Priscila de Oliveira Rosso[a], Jéssica Barbosa de Oliveira Gonçalves[c], Daniela Vieira Buchaim[a,c,d], Mizael Pereira[a], Jesus Carlos Andreo[a], Geraldo Marco Rosa Júnior[e,f], Bruna Botteon Della Coletta[a], João Vitor Tadashi Cosin Shindo[a], Rogério Leone Buchaim[a,c,*]

[a] Department of Biological Sciences (Anatomy), Bauru School of Dentistry, University of São Paulo (USP), Bauru, Brazil
[b] Universidad Iberoamericana (UNIBE), Santo Domingo, Dominican Republic
[c] Medical School, University of Marilia (UNIMAR), Marília, Brazil
[d] Medical School, University Center of Adamantina (UNIFAI), Adamantina, Brazil
[e] University of the Sacred Heart (USC), Bauru, Brazil
[f] University of the Ninth of July (UNINOVE), Bauru, Brazil

ARTICLE INFO

Keywords:
Bone regeneration
Bone repair
Alcohol
Biomaterial

ABSTRACT

This study evaluated the effect of ethanol on the repair in calvaria treated with beta-tricalcium phosphate (β-TCP). Forty rats were distributed into 2 groups: Water group (CG, n = 20) and Alcohol Group (AG, n = 20), which received 25% ethanol ad libitum after an adaptation period of 3 weeks. After 90 days of liquid diet, the rats were submitted to a 5.0 mm bilateral craniotomy in the parietal bones; the left parietal was filled with β-TCP (CG-TCP and AG-TCP) and the contralateral only with blood clot (CG-Clot and AG-Clot). The animals were killed after 10, 20, 40 and 60 days. The groups CG-Clot and AG-Clot showed similar pattern of bone formation with a gradual and significant increase in the amount of bone in CG-Clot (22.17 ± 3.18 and 34.81 ± 5.49) in relation to AG-Clot (9.35 ± 5.98 and 21.65 ± 6.70) in periods of 20–40 days, respectively. However, in the other periods there was no statistically significant difference. Alcohol ingestion had a negative influence on bone formation, even with the use of β-TCP, exhibiting slow resorption and replacement by fibrous tissue, with 16% of bone formation within 60 days in AG-TCP, exhibiting immature bone tissue with predominance of disorganized collagen fibers. Defects in CG-TCP showed bone tissue with predominance of lamellar arrangement filling 39% of the original defect. It can be concluded that chronic ethanol consumption impairs the ability to repair bone defects, even with the use of a β-TCP biomaterial.

1. Introduction

Alcohol is responsible for the deaths of 3.3 million people worldwide each year, 5.1% of which are related to the most varied diseases (Verhaeghe et al., 2017). Alcohol acts as a toxic element to vital organs, acting harmfully on tissue integrity even in resistant tissues as bones. These pathological effects trigger complications in the biological process of bone repair, and may cause delayed consolidation, pseudoarthroses and even non-union (Marsell and Einhorn, 2010).

The mechanisms of action of alcohol in bone are not fully elucidated, but studies report a decoupling between bone formation and resorption by indirect effects that interfere with bone homeostasis, such as decrease in testosterone, insulin-like growth factor 1(IGF-1), calcitonin, increased parathyroid hormone (PTH), interleukin-6 (IL-6), oncostatin M, cortisol and calcium excretion (Maurel et al., 2012).

Conversely, excessive and chronic alcohol consumption has direct effects on the activity of bone cells and their metabolites, including the increased synthesis of sclerostin by osteocytes, modulation of canonical

* Corresponding author at: Department of Biological Sciences (Anatomy), Bauru School of Dentistry, University of São Paulo (USP), Alameda Dr. Octávio Pineiro Brisola 9-75, Vila Nova Cidade Universitária, CEP 17012-901, Bauru, São Paulo, Brazil.
E-mail addresses: karinatorrespomini@gmail.com (K.T. Pomini), cestari@fob.usp.br (T.M. Cestari), irish_knaan@hotmail.com (Í.J. Santos German), marcelierosso@usp.br (M.P. de Oliveira Rosso), goncalvesjbo@yahoo.com.br (J.B. de Oliveira Gonçalves), danibuchaim@usp.br (D.V. Buchaim), mizael.pereira@usp.br (M. Pereira), jcandreo@usp.br (J.C. Andreo), geraldomrjr@yahoo.com.br (G.M. Rosa), brucoletta@hotmail.com (B.B. Della Coletta), jvshindo@gmail.com (J.V.T. Cosin Shindo), rogerio@fob.usp.br (R.L. Buchaim).

https://doi.org/10.1016/j.drugalcdep.2018.12.031
Received 12 September 2018; Received in revised form 3 December 2018; Accepted 10 December 2018
Available online 16 February 2019

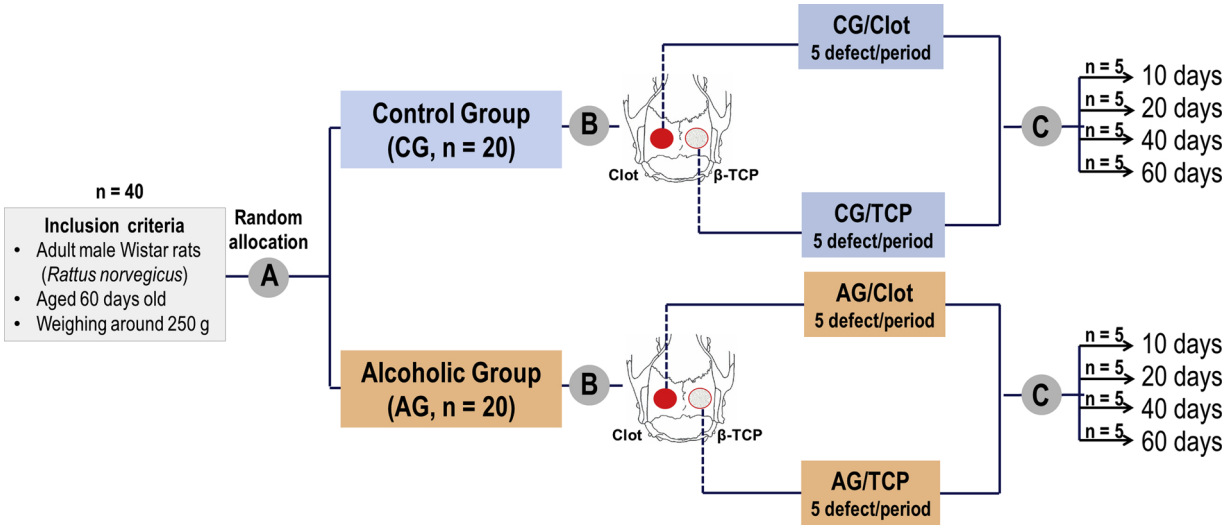

Fig. 1. Distribution of the animals into the Groups. A) Forty rats were divided into two groups: Non-alcoholic or control group (CG, n = 20) and Alcoholic group (AG, n = 20). **B)** After surgical procedures, four subgroups were preformatted according to treatment: CG-Clot (Control Group that received only water with liquid diet and the defect was filled with blood Clot), CG-TCP (Control Group that received only water with liquid diet and the defect was filled with β-TCP), AG-Clot (Alcoholic Group that received only ethanol solution 25% v/v with liquid diet and the defect was filled with blood clot), and AG-TCP (Alcoholic Group that received only ethanol solution 25% v/v with liquid diet and the defect was filled with β-TCP). **C)** Euthanasia period 10, 20, 40 and 60 days.

Wnt signaling pathway that is responsible for osteoblastic differentiation and maturation, increased concentration of TNF-α and IL-β that stimulate RANKL-RANK binding causing osteoclastic activation and osteoclastogenesis, and decreased synthesis of BMP, Wnt and OPG proteins by the osteoblasts responsible for bone formation (Chen et al., 2011; García-Valdecasas-Campelo et al., 2006; Jung, 2011 Maurel et al., 2012).

The bone tissue presents great sensitivity and high regenerative capacity; in many situations, it is able to perfectly restore its architectural bone structure and mechanical properties. However, this ability may not manifest or may fail in large bone defects and also under the influence of ethanol. In these cases, the bone tissue does not exhibit this spontaneous capacity, requiring reconstructive operative procedures including bone grafting as the main treatment technique (Caria et al., 2007; Hwang and Wang, 2007).

The autogenous bone grafts are still the “gold standard” in terms of bone regeneration because of their predictable outcomes based on osteoinduction, osteoconduction and osteogenic properties. However, there are limitations of autografts which include restricted donor sites and possible harvesting morbidity (Jensen et al., 2016; Nkenke and Neukam, 2014; Sakkas et al., 2017). Given these limitations, there is a great search for biomaterials as bone substitutes and reconstructive techniques to mimic the characteristics and clinical results of the autogenous bone (Delgado-Ruiz et al., 2015; Pilipchuk et al., 2015).

Among the various synthetic biomaterials, the granular bioceramics beta-tricalcium phosphate (β-TCP) is frequently used in orthopedic and dental surgeries for reconstruction of bone defects. It has good biocompatibility due to the similar mineral composition as human bone; it is resorbable, bioinert and presents high osteoconductive capacity, favoring the process of recognition and signaling of migratory cells originated by proliferation of the defect margin (Bellucci et al., 2016; Yang et al., 2014).

Despite the growing interest in the development of biomaterials that have adequate biological and physicochemical properties (Buchaim et al., 2007) and the increased rate of alcoholism worldwide, few studies have investigated the effects of alcohol abuse on the osseointegration of bone substitutes. Thus, this study evaluated the influence of chronic ethanol intake on the repair process of cranial bone defects filled with beta-tricalcium phosphate biomaterial.

2. Materials and methods

2.1. Bone graft substitutes

The Beta-Tricalcium Phosphate (ß-TCP) (Bionnovation Biomedical A.B., Brazil) evaluated in this study is a synthetic and resorbable microgranular ceramic, with particle size from 0.1 to 0.5 mm and conditioned in vial quantities of 0.5 g. It is made of Calcium Hydroxide ($Ca(OH)_2$) and Phosphoric Acid (H_3PO_4), whose Calcium Phosphate ($Ca_3(PO_4)_2$) proportion is of 91.67%, according to the X-Ray Diffraction Test, and presents 80% of pores between 0.33 to 0.72 µm (Mercury Intrusion Porosimetry Test). This dental product is registered in Brazilian Ministry of Health by The National Sanitary Surveillance Agency (ANVISA10392710019).

2.2. Experimental design

Forty adult male Wistar rats (*Rattus norvegicus*), aged 60 days old, weighing around 250 g, were used in this study. The animals were housed in cages (four/cage), fed a standard rat chow (Labina® - Purina, São Paulo, Brazil) and maintained in a room at constant temperature (20–22 °C) on a 12-hr light/dark cycle. All experimental procedures on the animals were conducted with the approval of the Institutional Review Board on Animal Studies of Bauru School of Dentistry, São Paulo State University (Protocol: CEEPA-022/2012).

Initially, the animals were randomly divided into two groups: non-alcoholic or control group (CG, n = 20) and alcoholic group (AG, n = 20). Animal health was monitored daily and body masses (g) measured in two periods (0 day and at euthanasia). After the surgical procedures, four subgroups were preformatted according to treatment: CG-Clot (Control Group that received only water with liquid diet and the defect was filled with blood Clot), CG-TCP (Control Group that received only water with liquid diet and the defect was filled with β-TCP), AG-Clot (Alcoholic Group that received only ethanol solution 25% v/v with liquid diet and the defect was filled with blood clot), and AG-TCP (Alcoholic Group that received only ethanol solution 25% v/v with liquid diet and the defect was filled with β-TCP) (Fig. 1).

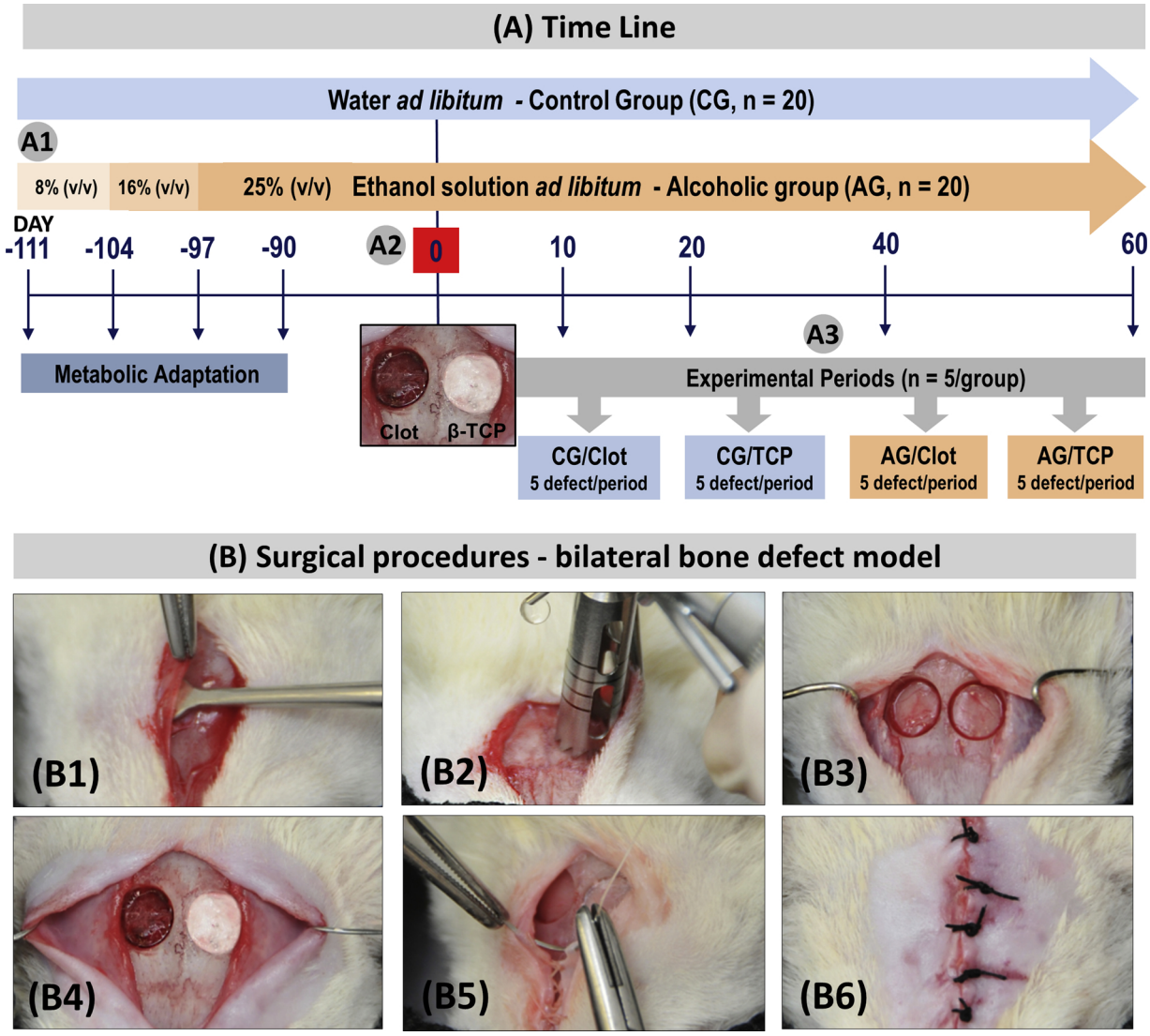

Fig. 2. Study design. A) Time line: A1) Forty rats were divided into two groups: Control group (CG) that received only water with liquid diet, and Alcoholic group (AG) that received ethanol solution 25% (v/v) with liquid diet after adaptation period of 21 days (-111 days to -90 days); A2) After 111 days for chronic alcohol modeling (0 day), two bone defects were created in the parietal bones; one defect was filled with blood clot and the other with β-TCP; and A3) at 10, 20, 40 and 60 days the skulls of 5 animals/group were collected, totalizing 5 defects/period of each subgroup CG-Clot, CG-TCP, AG-Clot and AG-TCP. **B) Surgical procedures – bilateral bone defect model:** B1) 20 mm- skin incision, divulsion of the subcutaneous and periosteum using an elevator; B2) Osteotomy using a 5mm- trephine bur; B3) two bone defects in parietal bones; B4) one defect filled with β-TCP and the contralateral only with blood clot; B5) Periosteum suture with nylon 5-0; B6) Tegument suture with 4-0 silk thread.

2.3. Chronic alcohol administration

The animals in the alcoholic group received aqueous ethanol solution as a liquid diet. For metabolic adaptation to alcohol, the animals received *ad libitum* a liquid diet containing ethanol 8% (v/v) in the first week, 16% (v/v) in the second week and 25% v/v in the third week (see Fig. 2A1). The dosage of 25% ethanol was maintained until the corresponding period of euthanasia (Buchaim et al., 2009; Buchaim et al., 2012). The control group received tap water as the liquid diet throughout the experiment.

2.4. Surgical procedures

All surgical procedures were performed at the Mesoscopic Laboratory - discipline of Anatomy (Bauru School of Dentistry, University of São Paulo, Brazil) by the same team of professionals, and only the surgeon was not aware of which treatment the animal belonged to.

After 111 days of chronic alcohol modeling (0 day) (see Fig. 2A2), all animals were anesthetized, under the same protocols, with ketamine at a dose of 50 mg / kg i.m. (Dopalen ™, Ceva, Paulínia, SP, Brazil) plus xylazine at a dose of 10 mg / kg i.m. (Anasedan ™, Ceva, Paulinia, SP, Brazil), with strict monitoring of anesthesia mainly in alcoholic animals (Flintoff, 2014; Newman et al., 1986).

The frontoparietal region was trichotomized and disinfected with polyvidone-iodine (Povidine™, Vic Pharma, Brazil). A 20-mm midsagittal incision was made through the skin. The periosteal tissue was carefully elevated from the parietal bones (Fig. 2B1). One 5-mm defect was created using trephine bur (Neodent, Curitiba, PR, Brazil) on both sides (Más et al., 2016; Qiu et al., 2007; Santana et al., 2016; Zong et al., 2010) (Fig. 2B2 – B3).

The defect in left parietal was filled with 15 mg β-TCP (previously established in a pilot study) homogenized with saline solution, sufficient to form a paste consistency, thus facilitating the condensation of particles, and the right parietal was filled only with blood clot (Fig. 2B4). The periosteum and tegument were repositioned and

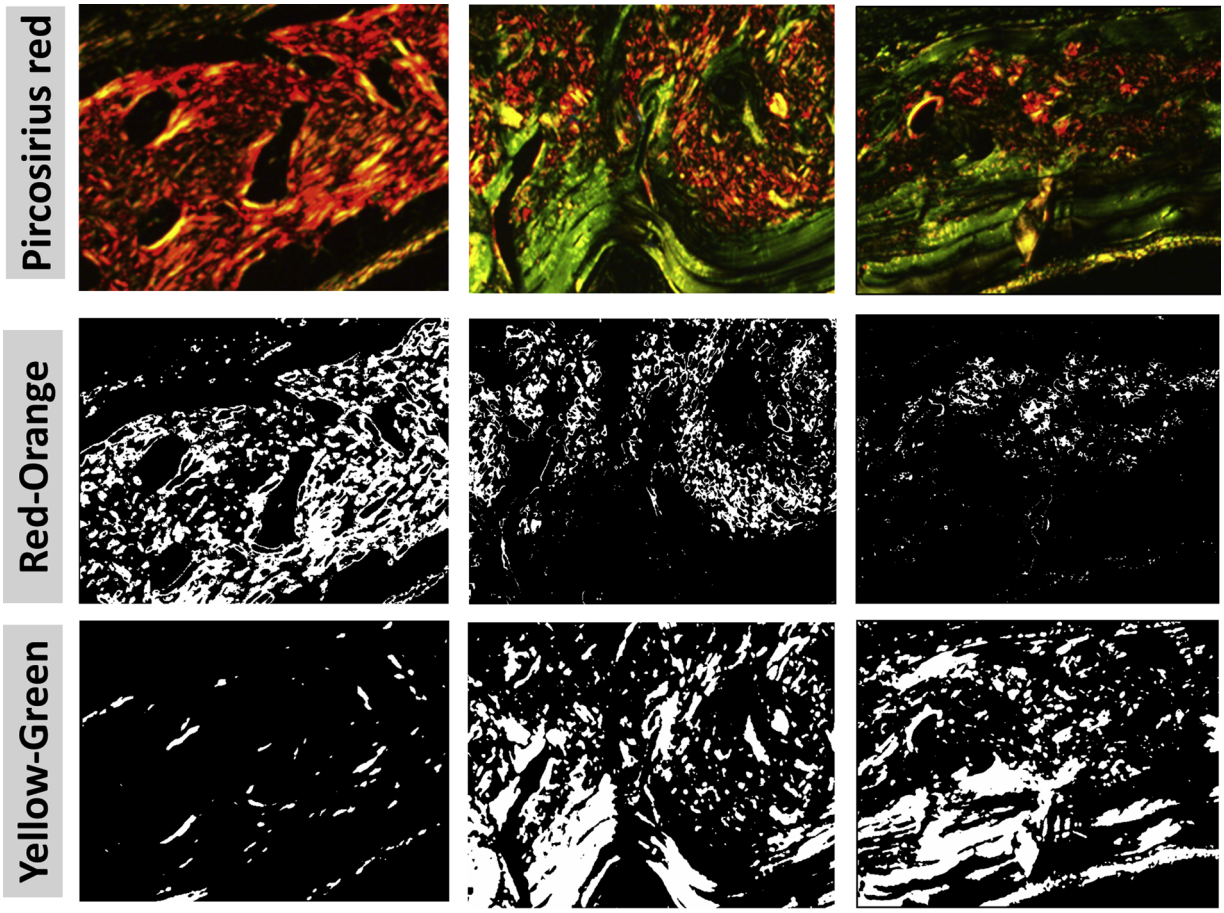

RGB color	Red- orange		Yellow-green	
	Low	High	Low	High
Red	75	255	54	255
Green	0	50	88	255
Blue	0	0	0	0

Fig. 3. Bone photomicrographies stained with picrosirius red obtained on the polarization microscope and calibration partners for evaluation of volume density (%) of the bone collagen fibers by RGB color red-orange and yellow-green (For interpretation of the references to colour in this figure legend, the reader is referred to the web version of this article).

sutured with nylon 5-0 (Mononylon™Somerville S.A) and silk 4-0 (Ethicon™ Johnson & Johnson Company), respectively (Fig. 2B5 – B6), to provide stability to the graft particles, decreasing the risk of soft tissue collapse (Neagu et al., 2016; Spicer et al., 2013).

The postoperative care consisted of a single intramuscular injection of enrofloxacin at a dose of 2.5 mg/Kg i.m. (Flotril™; Schering-Plough SA, Rio de Janeiro, Brazil) after surgical procedures and intramuscular injections of dipyrone at a dose of 0.06 mg/Kg (Analgex™; Agener União, São Paulo, Brazil) 12–24 h during 3 days.

2.5. Collection of samples and histological procedures

The animals were killed at the end of each trial period by anesthetic overdose. The parietal bones were removed, dissected and fixated in 10% buffered formalin for 48 h. The specimens were demineralized in EDTA, a solution containing 4.13% Titriplex™ III (Merck KGaA, Darmstadt, Germany) and 0.44% sodium hydroxide, for a period of approximately 40 days. Subsequently, the specimens were submitted to standard histological procedures for embedding in Histosec™(Merck KGaA, Darmstadt, Germany). Latero-lateral semi-serial 5-µm thick sections including the center of circular defects were obtained and stained with Hematoxylin and Eosin or Picrosirius Red.

2.6. Body mass analysis

Body mass measurement was obtained in two periods: the initial mass on the day of the surgical procedure (0 days - Fig. 2A2); and the final mass in the corresponding periods of euthanasia at 10, 20, 40 and 60 days (see Fig. 2A3). Mass gain and/or loss was calculated for each animal (final mass - initial mass). Measurement was performed on a Bel Mark 3500 precision scale (BEL® Analytical Equipment Ltda, São Paulo, Brazil), with maximum capacity of 3500 g and minimum of 200 g.

2.7. Histomorphometric evaluation

For slide analysis, the examiner was previously calibrated and

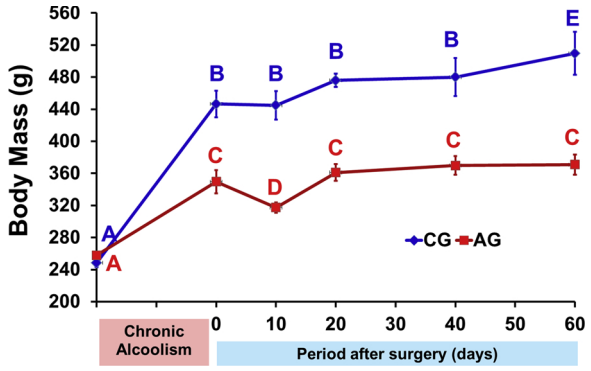

Fig. 4. Graphic evolution of body mass (g) during establishment of chronic alcoholism model (111 days) and bone repair periods, showing negative influence of alcohol consumption on the body mass of animals in AG compared to CG. Different letters $p < 0.05$ (two-way ANOVA showed interaction between group and period).

blinded with the use of masks in all evaluated slides, to avoid recognition of the type of treatment in each defect, group (water or alcohol) and experimental period. The histologic sections were analyzed in the Histology Laboratory of Bauru School of Dentistry, University of São Paulo (São Paulo, Brazil) by light microscopy (Olympus model BX50) at approximate magnifications of ×4, ×40 and ×100. To establish a standard criteria judgment, there was a training session with an experienced pathologist.

Histological analysis of sections stained with HE consisted of evaluative description of the bone repair process for each treatment (blood clot or ß-TCP) in different clinical conditions (non-alcoholic or alcoholic). For morphometric evaluation, two central sections stained with HE were used for quantification of newly formed bone areas using an image capture system (DP Controller software, Olympus, Tokyo, Japan). The total area (TA) to be analyzed corresponded to the entire area of the original surgical defect. This area was determined by first identifying the external and internal surfaces of the original calvarium at the right and left margins of the surgical defect, and then connecting them with lines drawn following their respective curvatures. The center of the histologic section (considering its total length) was located and 2.5 mm were measured to the right and to the left of this center point to determine the limits of the original surgical defect.

The total area (TA) and the newly formed bone area (A_{NFB}) were delineated in the Image J® Program, (Java-based image processing program developed at the National Institutes of Health, Image J™1.50d Wayne Rasband, National Institutes of Health, USA, Java 1.7_67; 64-bit) in pixels and converted into a percentage of the image by calculating the following relation: $P_{NFB} = A_{NFB} \times 100/_{TA}$ (P_{NFB} - newly formed bone percentage; A_{NFB} - newly formed bone area; TA - total area).

Sections stained with Picrosirius red were evaluated as to the quality of newly formed bone in the defects by structured collagen orientation. Thus, images were obtained from the defect using higher resolution digital camera Leica DFC 310FX (Leica™, Microsystems, Wetzlar, Germany) connected to confocal laser microscope Leica DM IRBE and capture system LAS 4.0.0 (Leica™, Microsystems, Heerbrugg, Switzerland).

To allow the identification and analysis of the quantity and quality of collagen by the birefringence of organization of fiber bundles, the central fields of the defects were analyzed under a polarized light microscope at 10x magnification. Three histological fields were captured corresponding to the entire extension of the defect and then the density area or percentage (%) area analysis of each fiber type per color was assessed using the image analysis software Axio Vision Rel. 4.8 Ink (Carl Zeiss MicroImaging GmbH, Jena, Deutschland). Woven bone was recognized by its random, unorganized fibrillar pattern, usually with polarization colors ranging from red-orange (poorly organized woven bone) and lamellar bone (bright green/yellow), depending on fiber width (see Fig. 3).

2.8. Statistical analysis

Data of body mass and bone volume per total tissue volume (BV/TV) were expressed as mean ± standard error of the mean (SEM). All tests were performed with Statistica software 10.0 (StatSoft Inc., Tulsa, OK, USA) and the significance level was established at $P < 0.05$. The Kolmogorov-Smirnov test was used to confirm that data were within the ranges of normal distribution in both groups. Two-way ANOVA and Tukey test were used to verify the possible interaction between groups and periods.

The influence of time on bone formation within each experimental group was analyzed by one-way ANOVA for independent samples and post hoc Tukey test. The *t*-test for independent samples was applied to evaluate possible interferences on bone formation associated with the clinical status of animals (non-alcoholic or alcoholic) for each treatment (clot or biomaterial). The paired "t" test was used to verify the interference of type of treatment (clot or biomaterial) on bone formation for each clinical condition (non-alcoholic or alcoholic) and each experimental period.

3. Results

3.1. Effect of ethanol on the general condition of rats

Throughout the study period all animals were in good general condition, and there were no significant differences between groups with regard to food consumption and water intake (data not shown). However, during the gradual induction of the alcoholism model (111 days) the body mass gain in ethanol-fed rats was smaller compared to control rats (Fig. 4). There was no noticeable difference in physical activity of ethanol-fed and control rats, but some animals showed signs of irritability and aggressiveness. There were no overt signs of morbidity and no mortality in the animals and no infections at the wound site or elsewhere after surgeries. In the control group, a gradual body mass gain was observed until 60 days, while in the ethanol-fed rats it remained constant throughout the experimental period with a significant reduction only at 10 days.

3.2. Histomorphometric comparisons between treatments (Clot vs. β-TCP) suggested a similar bone gain at 60 days for both treatments

In non-alcoholic rats (CG), the new bone formation started at the margins of craniotomies in both treatments, Clot (Figs. 5A and 6A) and β-TCP (Figs. 5B – 6B). Between 10–60 days, the bone deposition extended centripetally on the dura-mater surface. Graphically (Fig. 5E), greater bone formation was observed in CG-Clot than CG-TCP in the period between 20 and 60 days, with statistical differences at 20 days. In this endpoint, 60 days, a discontinuous layer of new bone formation was present along the dura-mater. The β-TCP materials were quickly resorbed until 10 days and replaced by connective tissue. Between 20–60 days some particles surrounded by resorptive cells with macrophages and foreign-body giant cells (FBGC) were present in the defect.

In alcoholic rats (AG), the new bone formation also started at the margins of craniotomies in both treatments, Clot (Figs. 5C – 6C) and β-TCP (Figs. 5D – 6D). However, the new bone formation was restricted to the margins of craniotomies throughout the experimental period (compare bone formation in Figs. 5C and D), except for AG-Clot at 60 days. Graphically (Fig. 5E) the period of higher bone accumulation in AG-Clot was 60 days (mean 25.7%), while in the AG-TCP the quantity of bone formation did not show differences between periods (mean 16%). In relation to groups, bone formation was in average 8.7% higher in AG/Clot than AG-TCP between 20–60 days. The large amount of β-

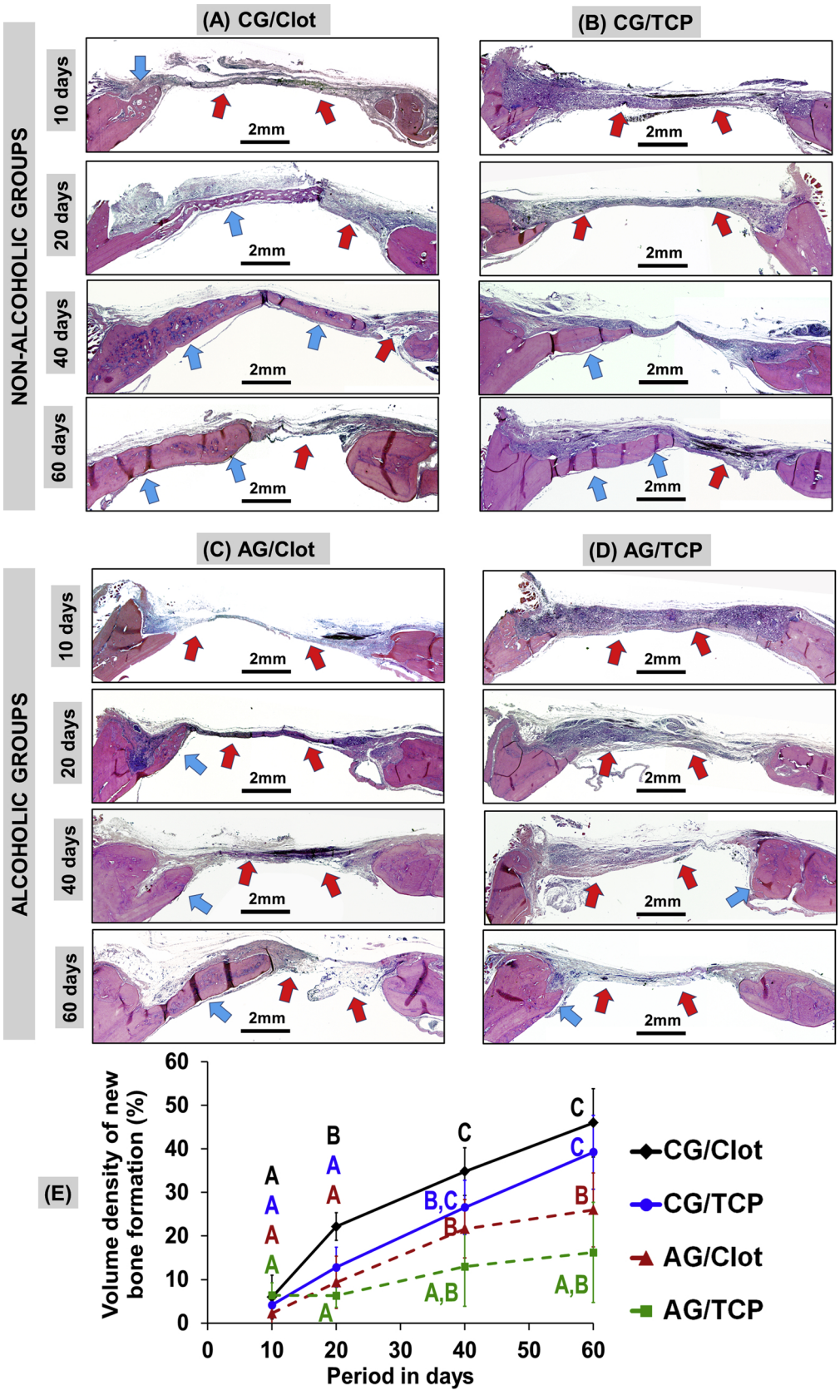

Fig. 5. Panoramic histological views (A–D) and graph of volume density of newly formed bone (E) in skull defects created in the animals. Non-Alcoholic (A–B) and Alcoholic (C–D) treated with Clot or β-TCP at different experimental periods. A–B) **Non-Alcoholic Groups** showed bone formation (blue arrows) occurring from the defect margin (B) and on the dura-mater surface. At 60 days, both treatment groups showed similar bone formation covering a greater part of the dura-mater surface and a small region filled with fibrous connective tissue and/or biomaterials (red arrows). C–D) **Alcoholic Groups** showed a discrete bone growth (blue arrows) on the defect border until 40 days. At 60 days, a large part of the defect was filled by connective tissue and/or β-TCP (red arrows), but in AG-Clot greater bone formation than AG-TCP defect could be observed. E) **Graph of newly formed bone** showed smaller bone formation in alcoholic group (AG-Clot and AG-TCP) than non-alcoholic group (CG-Clot and CG-TCP). N = 5/group and periods, different letters $p < 0.05$ between periods/group and groups/period. (HE; original magnification x 4; bar = 2 mm) (For interpretation of the references to colour in this figure legend, the reader is referred to the web version of this article).

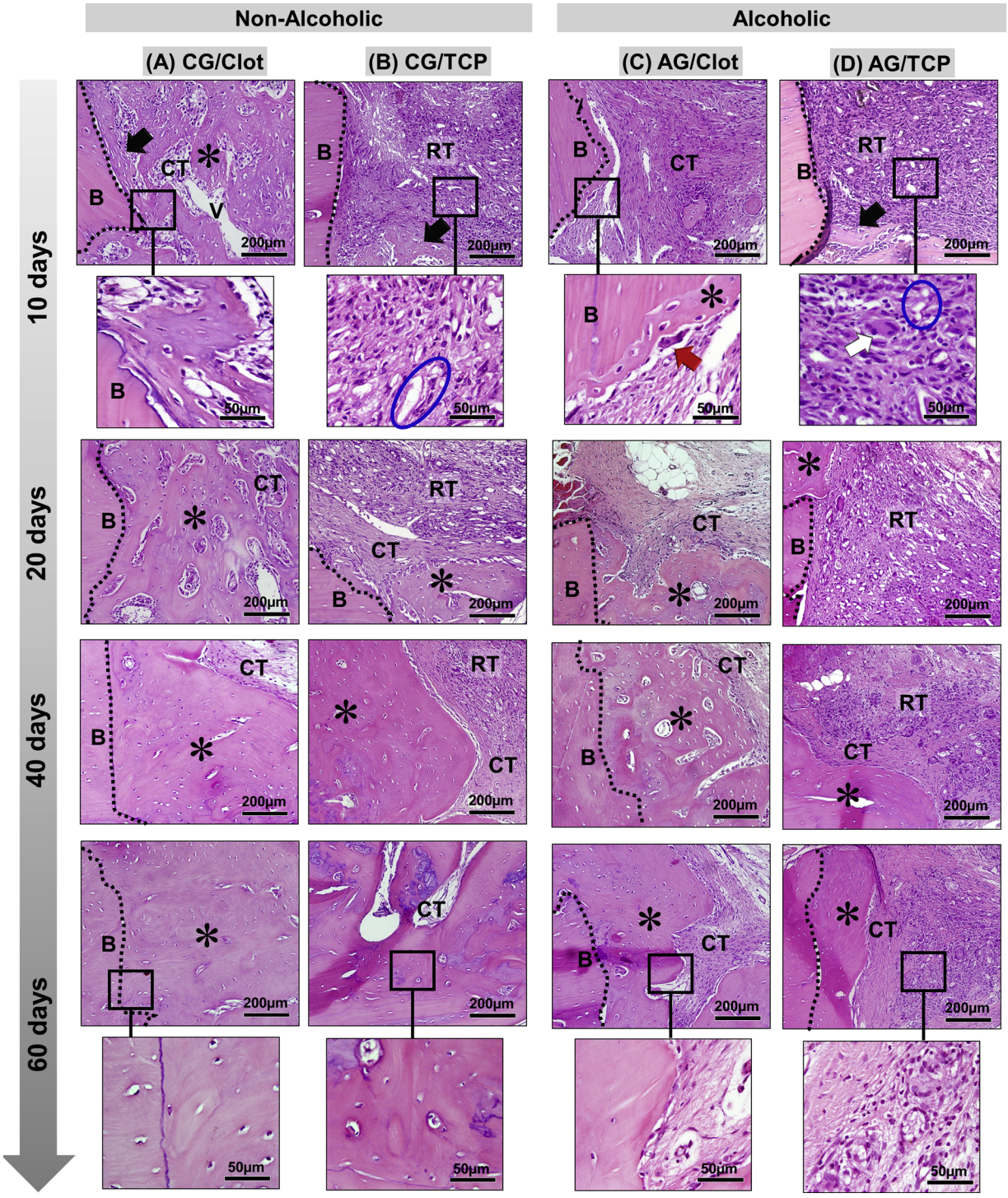

Fig. 6. Details of evolution of bone healing of skull defects created in the Non-Alcoholic and Alcoholic animals treated with Clot or TCP. **A) CG-Clot:** at 10 days, the defect showed trabecular bone formation (asterisks) adjacent to the defect border (B) and spaces between trabeculae filled by richly vascularized (V) connective tissue (CT) at 10 days. Between 20–60 days, the new bone showed gradual increase in thickness of trabeculae, leading to a compact structure until 60 days. **B) CG-TCP:** At 10 days, the defect was filled by β-TCP particles (inside the blue lined area) surrounded by connective tissue with some inflammatory cells. Between 20–60 days, the new bone formation increased with decrease of β-TCP particles and inflammatory response. At 60 days, compact bone formation with entrapment of some β-TCP particles was present on the defect border. **C) AG-Clot:** Small bone formation on the defect border and osteoclastic resorption (red arrow) were present at 10 days. After 20 days, a dense bone formation was present on the border and increased until 60 days. **D) AG-TCP** at 10 days, the defect was filled by small particles of β-TCP (inside the blue lined area) surrounded by a reactional tissue (RT) containing intense foreign body-type inflammatory process containing macrophages and multinucleated giant cells (white arrow). Between 30–60 days, β-TCP and inflammatory process decreased, but did not disappear and only a small bone formation was present on the lesion border at 60 days. (HE; original magnification x 20; bar = 200 μm; and Insets, magnified images x100; bar = 50 μm) (For interpretation of the references to colour in this figure legend, the reader is referred to the web version of this article).

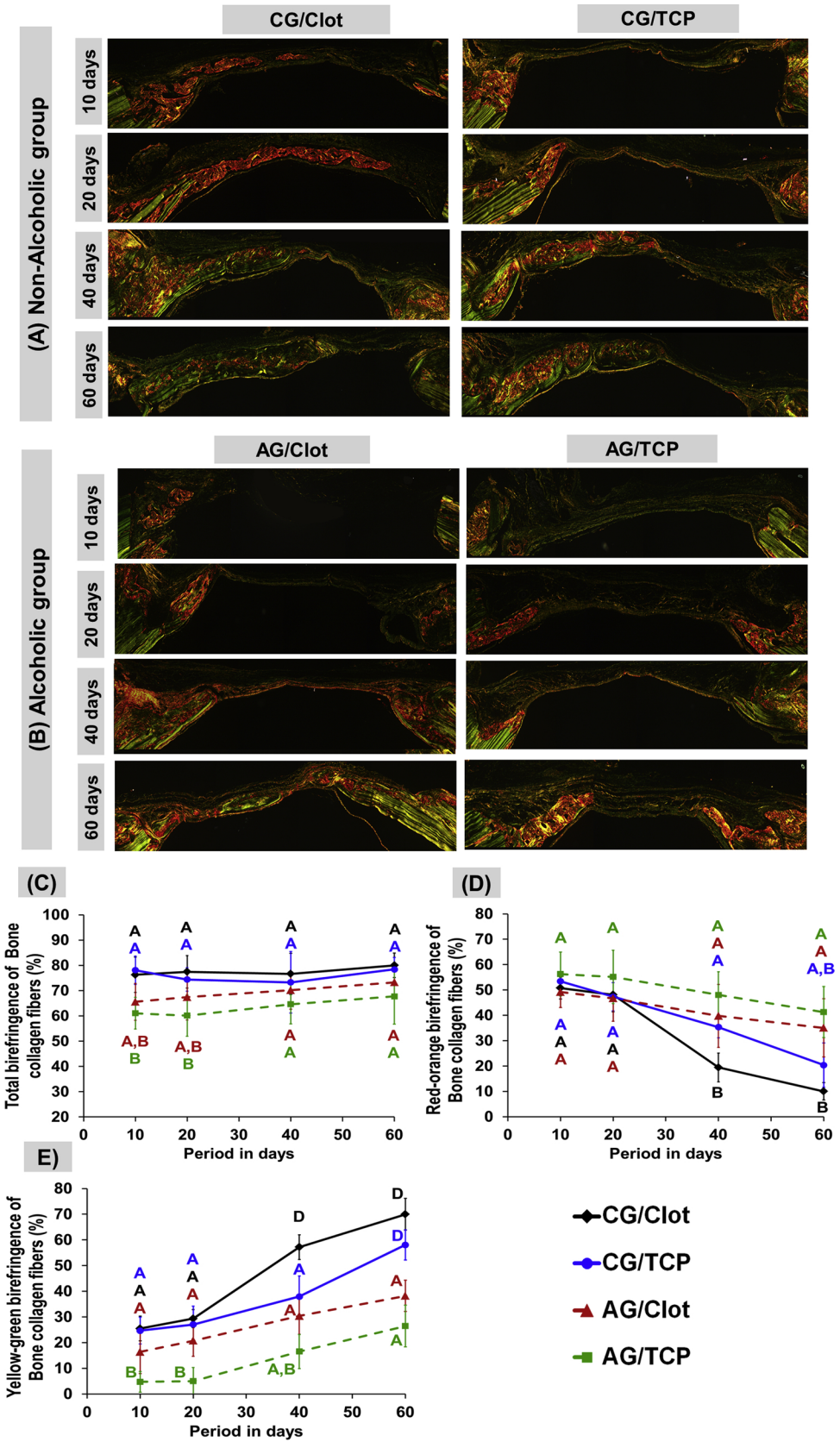

Fig. 7. Photomicrographies of birefringent fibers stained with Picrosirius red under polarized light at 10, 20, 40 and 60 days of repair: The red-**orange** birefringence color was observed in the immature bone formation containing thin and disorganized collagen fibers, which prevailed at initial repair periods (10 and 20 days); yellow-**green** color in the birefringence analysis was associated with lamellar/mature bone. Note a higher presence of yellow-**green** fibers/mature bone in non-alcoholic defects than alcoholic groups. The alcoholic defects filled with β-TCP showed a predominance of red-**orange** fibers/immature bone at 60 days. Original magnification x20. Bar = 100. Graphs of Area density/Percentage of birefringence color in the bone tissue for each group showed slower bone maturation in bone defects of alcoholic animals compared to Non-Alcoholic. The small bone maturation in the alcoholic group was more evident in those treated with biomaterials (β-TCP). N = 5, Bar = Standard deviation and different letters $p < 0.05$ between periods/group (ANOVA) and groups/period ("t" test) (For interpretation of the references to colour in this figure legend, the reader is referred to the web version of this article).

TCP materials was present at 10 and 20 days surrounded by many resorptive cells, FBGC and macrophages, characterizing a chronic inflammatory process.

3.3. Histomorphometric comparison between clinical conditions (alcoholic vs non-alcoholic) suggested a negative effect of alcohol consumption on bone formation

In the defect treated with blood clot, the bone formation pattern was similar between non-alcoholic and alcoholic conditions (compare the Fig. 5A and C), but the quantity of bone tissue (Fig. 5E) was significantly smaller in AG-Clot compared to CG-Clot at 40 and 60 days.

In the defect treated with β-TCP, an evident negative influence of alcohol on bone formation and β-TCP material resorption was observed (compare Fig. 5B with D). Graphically, only 16% of the defect was filled by bone tissue in alcoholic rats at 60 days, while in non-alcoholic animals the new bone percentage was 39%.

3.4. Picrosirius red staining showed less bone collagen organization/maturation in non-alcoholic defects treated with β-TCP

Representative images of Picrosirius red staining and graphs of area density or percentage of birefringence color in the bone tissue (Fig. 7) showed similar predominance of red-orange birefringence in all groups at 10 and 20 days (mean 50.9%) referring to the presence of immature bone. In these periods, the yellow-green fibers and total birefringence of bone collagen fibers were smaller in AG-TCP (4.75% and 67.7%, respectively) than in other groups (mean 24% and 77.3%, respectively), suggesting a small and slow bone formation in this group.

Between 20–60 days, in defects of non-alcoholic rats (CG-Clot and CG-TCP) the red-orange birefringence gradually decreased (mean 52.1%–15.9%) while yellow-green birefringence increased proportionally (mean 25.1%–64%) associated with the presence of lamellar/mature bone. In alcoholic groups (AG-Clot and AG-TCP), similar quantity of red-orange birefringence (mean 32.8%) and yellow-green birefringence (mean 32.5%) was present at 60 days associated with an immature bone tissue.

4. Discussion

Chronic alcoholism directly interferes with bone metabolism leading to osteopenia (Chakkalakal, 2005), increased predisposition to fractures and pseudoarthroses (Calori et al., 2007; Giannoudis et al., 2011; Gómez-Barrena et al., 2015). However, few studies report its influence on the bone repair process associated with biomaterials. Among them, beta-tricalcium phosphate has been considered a substitute biomaterial for autograft with satisfactory osteoconductive characteristic (Bizenjima et al., 2016; Taniyama et al., 2013).

Although β-TCP is considered a biocompatible bone substitute, it was not able to completely regenerate the intraosseous defect performed in this study as observed by Ramalingam et al. (2016), and also did not minimize the deleterious effects of alcohol already shown in the bone tissue.

Alcohol consumption negatively affected body mass gain throughout the experimental period (Budzik et al., 2017). Previous studies have reported that this is due to the decrease in total calorie intake required to maintain the body weight of the young adult rat (40–45 kcal / day / 300 g), as well as the dissipation of energy resulting from alcohol oxidation (Trevisiol et al., 2007). Alcohol and its metabolites can also modify the absorption and/or utilization of nutrients provided by foods and increase the energy expenditure at rest inducing thermogenesis (de Deco et al., 2015; Johnson et al., 1990; Maddalozzo et al., 2009; Maurel et al., 2011; Sreenathan et al., 1984).

Changes in body mass in alcoholic animals were more pronounced in the postoperative period related to convalescence, decreased food intake and movement capacity, as reported in experimental and clinical studies (Bradley et al., 2011; Lauing et al., 2009; Tonnesen, 2003).

The defects created in calvaria of rats, even in the groups that did not ingest alcohol and had the surgical cavities filled with blood clot, did not show total repair of the defect in the final period of 60 days, agreeing with studies that reported that this is a critical defect (Bizenjima et al., 2016; Cacciafesta et al., 2001; Gao et al., 2018; Lutolf et al., 2003; Qiu et al., 2007; Verna et al., 2002; Winn et al., 1999).

In the present study, no invasion of epithelial tissue from the areas adjacent to the defect was observed in all animals analyzed, and only one surgical cavity was circumscribed by fibrous connective tissue coming from the edges of the defect, which is a typical feature in the bone repair process of critical size defects surgically created in calvaria of rats. Thus, immediate repositioning of the periosteum and its suture decrease the risk of collapse of the tissues overlying the wound, precluding the appearance of fibrous connective tissue (Neagu et al., 2016; Spicer et al., 2013).

Histologically, at 10 days, all experimental groups showed a large amount of connective tissue and discrete bone formation. These results were consistent with studies that stated that neoformation started at the defect margins, probably stimulated by inflammatory, angiogenic and growth factors, and cell differentiation released in this region due to vascular rupture resulting from the surgical procedure and the adjacent presence of periosteum (Cestari et al., 2009; Dym et al., 2012; Hsiong and Mooney, 2006; Kanczler, 2008; Rocha et al., 2014; Zong et al., 2010).

The CG-Clot group, considered control in this experiment, initially showed new bone formation from the defect margins and followed the dura mater with a trabecular and immature arrangement, becoming lamellar and compact at 60 days. These results are expected in the physiological process of bone repair in the present model. However, implantation of a biomaterial in surgical defects triggers an initial inflammatory response of biological accommodation (Aamodt and Grainger, 2016). The influence of factors such as the implantation of biomaterials (Aamodt and Grainger, 2016), alcohol exposure (Karavitis and Kovacs, 2011) or smoking (Buchaim et al., 2018; Carroll et al., 2009) may be determinant in the type of repair following craniotomy, as in the prognosis of its recovery (Anderson et al., 2008; Klopfleisch, 2016).

Initially, at the 10- and 20-day periods, the AG-TCP and CG-TCP groups presented inflammatory cells involving β-TCP particles, an inherent cellular mechanism in the implantation of biomaterials in in vivo tissues (Jones et al., 2004; Karavitis and Kovacs, 2011). At 40 and 60 days, a decrease in inflammation was gradually observed in CG-TCP due to the biodegradation of β-TCP particles by phagocytic cells and an increase in new bone formation (Kunert-Keil et al., 2015; Marins et al., 2004; Schmidlin et al., 2013).

However, the AG-TCP group showed foci of reactive tissue up to 60 days, close to the graft, accompanied by clusters of macrophages and multinucleated giant cells (FBGC), in an attempt to contain persistent biomaterial particles and discrete bone formation at the defect border (Trevisiol et al., 2007; Zhu et al., 2015). The presence of these cells, as well as foreign body-type inflammatory reaction, are known to strongly inhibit the new bone formation. This observation was probably due to the negative influence of alcohol on the mechanisms of phagocytosis control by inflammatory macrophages, impairing the degradation process of the biomaterial (Camilli et al., 2004; Chakkalakal et al., 2002; Cook, 1998; Karavitis and Kovacs, 2011; Messingham et al., 2002; Napolitano et al., 1995; Soares et al., 2010).

At completion of the experiment (60 days) it was possible to observe the presence of β-TCP independent of the liquid diet used in the animals (non-alcoholic group and alcoholic group). These data are corroborated by the study of Trevisiol et al. (2007), who tested demineralized allogenic bone matrix (DABM) in rat model for chronic alcohol abuse.

The histomorphometric analysis of defects treated with clot revealed a gradual and significant increase in bone density in the CG-Clot group (22:17 ± 3.18 and 34.81 ± 5:49) compared to Ag-Clot

(9:35 ± 5.98 and 21.65 ± 6.70) in periods of 20–40 days, respectively (dos S. Kotake et al., 2015). In groups with defects treated with biomaterial, in the AG-TCP, the negative influence of alcohol on bone formation in all periods was noticeable, being evident at 60 days, with an average of 16% of the defect filled with bone tissue compared to 39% for the CG-TCP. Similar results were reported by Camilli et al. (2004) in calvaria of alcoholic rats, which presented smaller new bone formation near the hydroxyapatite particles in all analyzed periods.

Regarding the histochemical analysis of collagen fibers by picrosirius red staining, in the early periods it was possible to observe predominance of type III fibers, which were fine and disorganized in all experimental groups. As bone maturation occurs, there is predominance of type I fibers, which makes up 90% of the organic bone matrix (Florencio-silva et al., 2015). Thus, the effects of chronic alcohol consumption on bone metabolism inhibit the collagen synthesis by osteoblasts, and increase the degradation rate of type I collagen due to the increased concentration of collagenases with consequent deterioration of bone microarchitecture (Anderson et al., 2008; Araujo et al., 2014; Ciapetti et al., 1996; Kupraszewicz and Brzóska, 2013).

In summary, the synthetic biomaterials used for replacement and regeneration of the bone structure have attracted the attention of several research groups because it is a promising alternative to the existing treatments. For prospective studies requiring repair of large bone defects and a systemic impairment caused by alcoholism, analysis of noninvasive complementary treatments such as low power laser (LLLT) or low intensity pulsed ultrasound (LIPUS) (de Oliveira Gonçalves et al., 2016; Pomini et al., 2014) is suggested.

5. Conclusion

Based on the experimental model used, it can be concluded that chronic ethanol consumption negatively interferes with the bone defect repair capacity, even with the use of a β-TCP biomaterial.

Role of funding source

Contributors section - including the author's statement of approval of the final manuscript.

Conflict of interest

There was no conflict of interest.

Acknowledgements

This study was financed in part by the Coordenação de Aperfeiçoamento de Pessoal de Nível Superior - Brasil (CAPES) - Finance Code 001. The content is solely the responsibility of the authors and does not necessarily represent the official views of the funding agencies.

Appendix A. peer-reviewed paper in Drug and Alcohol Dependence

Supplementary material related to this article can be found, in the online version, at doi:https://doi.org/10.1016/j.drugalcdep.2018.12.031.

References

Aamodt, J.M., Grainger, D.W., 2016. Extracellular matrix-based biomaterial scaffolds and the host response. Biomaterials 86, 68–82. https://doi.org/10.1016/j.biomaterials.2016.02.003.

Anderson, J.M., Rodriguez, A., Chang, D.T., 2008. Foreign body reaction to biomaterials. Semin. Immunol. 20, 86–100. https://doi.org/10.1016/j.smim.2007.11.004.

Araujo, C.M., de Johann, A.C.B.R., Camargo, E.S., Tanaka, O.M., 2014. The effects of binge-pattern alcohol consumption on orthodontic tooth movement. Dental Press J. Orthod. 19, 93–98. https://doi.org/10.1590/2176-9451.19.6.093-098.oar.

Bellucci, D., Sola, A., Cannillo, V., 2016. Hydroxyapatite and tricalcium phosphate composites with bioactive glass as second phase: state of the art and current applications. J. Biomed. Mater. Res. - A 104, 1030–1056. https://doi.org/10.1002/jbm.a.35619.

Bizenjima, T., Takeuchi, T., Seshima, F., Saito, A., 2016. Effect of poly (lactide-co-glycolide) (PLGA)-coated beta-tricalcium phosphate on the healing of rat calvarial bone defects: a comparative study with pure-phase beta-tricalcium phosphate. Clin. Oral Implants Res. 27, 1360–1367. https://doi.org/10.1111/clr.12744.

Bradley, K.A., Rubinsky, A.D., Sun, H., Bryson, C.L., Bishop, M.J., Blough, D.K., Henderson, W.G., Maynard, C., Hawn, M.T., Tønnesen, H., Hughes, G., Beste, L.A., Harris, A.H.S., Hawkins, E.J., Houston, T.K., Kivlahan, D.R., 2011. Alcohol screening and risk of postoperative complications in male VA patients undergoing major noncardiac surgery. J. Gen. Intern. Med. 26, 162–169. https://doi.org/10.1007/s11606-010-1475-x.

Buchaim, R.L., Goissis, G., Andreo, J.C., Roque, D.D., Roque, J.S., Buchaim, D.V., Rodrigues, A.C., 2007. Biocompatibility of anionic collagen matrices and its influence on the orientation of cellular growth. Cienc. Odontol. Bras. 10, 12–20. https://doi.org/10.14295/bds.2007.v10i3.272.

Buchaim, R.L., Buchaim, D.V., Andreo, J.C., Roque, D.D., Roque, J.S., Rodrigues, A.C., 2009. Efeitos de 03 dietas alcoólicas na reparação óssea em tíbia de ratos. Cienc. Odontol. Bras. 12, 17–23. https://doi.org/10.14295/bds.2009.v12i2.346.

Buchaim, R.L., Andreo, J.C., Rodrigues, A., de, C., Buchaim, D.V., Roque, D.D., Roque, J.S., Rosa Junior, G.M., 2012. Bovine Bone Matrix Action Associated With Morphogenetic Protein in Bone Defects in Rats Submitted to Alcoholism. Int. J. Morphol. 30, 266–271.

Buchaim, D.V., Dos Santos Bueno, P.C., Andreo, J.C., Roque, D.D., Roque, J.S., Zilio, M.G., Salatin, J.A., Kawano, N., Furlanette, G., Buchaim, R.L., 2018. Action of a deproteinized xenogenic biomaterial in the process of bone repair in rats submitted to inhalation of cigarette smoke. Acta Cir. Bras. 33, 324–332. https://doi.org/10.1590/s0102-865020180040000004.

Budzik, J.F., Lefebvre, G., Behal, H., Verclytte, S., Hardouin, P., Teixeira, P., Cotten, A., 2017. Bone marrow perfusion measured with dynamic contrast enhanced magnetic resonance imaging is correlated to body mass index in adults. Bone 99, 47–52. https://doi.org/10.1016/j.bone.2017.03.048.

Cacciafesta, V., Dalstra, M., Bosch, C., Melsen, B., Andreassen, T.T., 2001. Growth hormone treatment promotes guided bone regeneration in rat calvarial defects. Eur. J. Orthod. 23, 733–740. https://doi.org/10.1093/ejo/23.6.733.

Calori, G.M., Albisetti, W., Agus, A., Iori, S., Tagliabue, L., 2007. Risk factors contributing to fracture non-unions. Injury 38. https://doi.org/10.1016/S0020-1383(07)80004-0.

Camilli, J.A., Da Cunha, M.R., Bertran, C.A., Kawachi, E.Y., 2004. Subperiosteal hydroxyapatite implants in rats submitted to ethanol ingestion. Arch. Oral Biol. 49, 747–753. https://doi.org/10.1016/j.archoralbio.2004.02.009.

Caria, P.H.F., Kawachi, E.Y., Bertran, C.A., Camilli, J.A., 2007. Biological assessment of porous-implant hydroxyapatite combined with periosteal grafting in maxillary defects. J. Oral Maxillofac. Surg. 65, 847–854. https://doi.org/10.1016/j.joms.2006.05.059.

Carroll, M.E., Anker, J.J., Perry, J.L., 2009. Modeling risk factors for nicotine and other drug abuse in the preclinical laboratory. Drug Alcohol Depend. 104, 70–78. https://doi.org/10.1016/j.drugalcdep.2008.11.011.

Cestari, T.M., Granjeiro, J.M., De Assis, G.F., Garlet, G.P., Taga, R., 2009. Bone repair and augmentation using block of sintered bovine-derived anorganic bone graft in cranial bone defect model. Clin. Oral Implants Res. 20, 340–350. https://doi.org/10.1111/j.1600-0501.2008.01659.x.

Chakkalakal, D.A., 2005. Alcohol-induced bone loss and deficient bone repair. Alcohol. Clin. Exp. Res. 29, 2077–2090. https://doi.org/10.1097/01.alc.0000192039.21305.55.

Chakkalakal, Da, Novak, J.R., Fritz, E.D., Mollner, T.J., McVicker, D.L., Lybarger, D.L., McGuire, M.H., Donohue, T.M., 2002. Chronic ethanol consumption results in deficient bone repair in rats. Alcohol Alcohol. 37, 13–20. https://doi.org/10.1093/alcalc/37.1.13.

Chen, H., Gilbert, L.C., Lu, X., Liu, Z., You, S., Weitzmann, M.N., Nanes, M.S., Adams, J., 2011. A new regulator of osteoclastogenesis: estrogen response element-binding protein in bone. J. Bone Miner. Res. https://doi.org/10.1002/jbmr.456.

Ciapetti, G., Verri, E., Granchi, D., Cenni, E., Gamberini, S., Benetti, D., Mian, M., Pizzoferrato, A., 1996. In vitro assessment of phagocytosis of bovine collagen by human monocytes/macrophages using a spectrophotometric method. Biomaterials 17, 1703–1707. https://doi.org/10.1016/0142-9612(96)87650-2.

Cook, R.T., 1998. Alcohol abuse, alcoholism, and damage to the immune system - A review. Alcohol. Clin. Exp. Res. 22, 1927–1942. https://doi.org/10.1097/00000374-199812000-00007.

de Deco, C.P., da Silva Marchini, A.M.P., Marchini, L., da Rocha, R.F., 2015. Extended periods of alcohol intake negatively affects osseointegration in rats. J. Oral Implantol. 41, e44–9. https://doi.org/10.1563/AAID-JOI-D-13-00111.

de Oliveira Gonçalves, J.B., Buchaim, D.V., de Souza Bueno, C.R., Pomini, K.T., Barraviera, B., Júnior, R.S.F., Andreo, J.C., de Castro Rodrigues, A., Cestari, T.M., Buchaim, R.L., 2016. Effects of low-level laser therapy on autogenous bone graft stabilized with a new heterologous fibrin sealant. J. Photochem. Photobiol. B, Biol. 162, 663–668. https://doi.org/10.1016/j.jphotobiol.2016.07.023.

Delgado-Ruiz, R.A., Calvo Guirado, J.L., Romanos, G.E., 2015. Bone grafting materials in critical defects in rabbit calvariae. A systematic review and quality evaluation using ARRIVE guidelines. Clin. Oral Implants Res. 1–15. https://doi.org/10.1111/clr.12614.

dos S. Kotake, B., Salzedas, L., Ervolino, E., Calzzani, R., Sebald, W., Issa, J., 2015. Bone recuperation after rhBMP-2 insertion in alcoholic animals-experimental study. Curr. Pharm. Des. 21, 3557–3564. https://doi.org/10.2174/1381612821666150428163307.

Dym, H., Huang, D., Stern, A., 2012. Alveolar bone grafting and reconstruction procedures prior to implant placement. Dent. Clin. North Am. 56, 209–218. https://doi.

org/10.1016/j.cden.2011.09.005.
Flintoff, K., 2014. Oh rats! A guide to rat anaesthesia for veterinary nurses and technicians. N Z Vet Nurse 20, 22–27.
Florencio-silva, R., Rodrigues, G., Sasso-cerri, E., Simões, M.J., Cerri, P.S., Cells, B., 2015. Biology of bone tissue : structure, function, and factors that influence bone cells. Biomed Res. Int. 2015. https://doi.org/10.1155/2015/421746.
Gao, R., Watson, M., Callon, K.E., Tuari, D., Dray, M., Naot, D., Amirapu, S., Munro, J.T., Cornish, J., Musson, D.S., 2018. Local application of lactoferrin promotes bone regeneration in a rat critical-sized calvarial defect model as demonstrated by micro-CT and histological analysis. J. Tissue Eng. Regen. Med. 12, e620–e626. https://doi.org/10.1002/term.2348.
García-Valdecasas-Campelo, E., González-Reimers, E., Santolaria-Fernández, F., De la Vega-Prieto, M.J., Milena-Abril, A., Sánchez-Pérez, M.J., Martínez-Riera, A., De Los Ángeles Gómez-Rodríguez, M., 2006. Serum osteoprotegerin and rankl levels in chronic alcoholic liver disease. Alcohol Alcohol. 41, 261–266. https://doi.org/10.1093/alcalc/agl004.
Giannoudis, P.V., Jones, E., Einhorn, T.A., 2011. Fracture healing and bone repair. Injury 42, 549–550. https://doi.org/10.1016/j.injury.2011.03.037.
Gómez-Barrena, E., Rosset, P., Lozano, D., Stanovici, J., Ermthaller, C., Gerbhard, F., 2015. Bone fracture healing: Cell therapy in delayed unions and nonunions. Bone 70, 93–101. https://doi.org/10.1016/j.bone.2014.07.033.
Hsiong, S.X., Mooney, D.J., 2006. Regeneration of vascularized bone. Periodontology 2000 (41), 109–122. https://doi.org/10.1111/j.1600-0757.2006.00158.x.
Hwang, D., Wang, H.L., 2007. Medical contraindications to implant therapy: part II: relative contraindications. Implant Dent. 16, 13–23. https://doi.org/10.1097/ID.0b013e31803276c8.
Jensen, A.T., Jensen, S.S., Worsaae, N., 2016. Complications related to bone augmentation procedures of localized defects in the alveolar ridge. A retrospective clinical study. Oral Maxillofac. Surg. 20, 115–122. https://doi.org/10.1007/s10006-016-0551-8.
Johnson, D.H., Kimura, R.E., Galinsky, R.E., 1990. New chronic gastric cannula for feeding ethanol liquid diet to young and old rats. J. Pharmacol. Methods 24, 37–42. https://doi.org/10.1016/0160-5402(90)90047-O.
Jones, J.A., Dadsetan, M., Collier, T.O., Ebert, M., Stokes, K.S., Ward, R.S., Hiltner, P.A., Anderson, J.M., 2004. Macrophage behavior on surface-modified polyurethanes. J. Biomater. Sci. Polym. Ed. 15, 567–584. https://doi.org/10.1163/156856204323046843.
Jung, M.K., 2011. Alcohol exposure and mechanisms of tissue injury and repair. Alcohol. Clin. Exp. Res. 35, 392–399. https://doi.org/10.1111/j.1530-0277.2010.01356.x. Alcohol.
Kanczler, J.M., 2008. Osteogenesis and angiogenesis: the potential for engineering bone. Eur. Cell. Mater. 100–114. https://doi.org/10.22203/eCM.v015a08.
Karavitis, J., Kovacs, E.J., 2011. Macrophage phagocytosis: effects of environmental pollutants, alcohol, cigarette smoke, and other external factors. J. Leukoc. Biol. 90, 1065–1078. https://doi.org/10.1189/jlb.0311114.
Klopfleisch, R., 2016. Macrophage reaction against biomaterials in the mouse model – phenotypes, functions and markers. Acta Biomater. 43, 3–13. https://doi.org/10.1016/j.actbio.2016.07.003.
Kunert-Keil, C., Scholz, F., Gedrange, T., Gredes, T., 2015. Comparative study of biphasic calcium phosphate with beta-tricalcium phosphate in rat cranial defects-A molecular-biological and histological study. Ann. Anat. 199, 79–84. https://doi.org/10.1016/j.aanat.2013.12.001.
Kupraszewicz, E., Brzóska, M.M., 2013. Excessive ethanol consumption under exposure to lead intensifies disorders in bone metabolism: a study in a rat model. Chem. Biol. Interact. 203, 486–501. https://doi.org/10.1016/j.cbi.2013.01.002.
Lauing, K., Himes, R., Rachwalski, M., Strotman, P., John, J., 2009. Binge Alcohol Treatment of Adolescent Rats Site-Specific Differences in Bone Loss and Incomplete 42, 649–656. https://doi.org/10.1016/j.alcohol.2008.08.005.BINGE.
Lutolf, M.P., Weber, F.E., Schmoekel, H.G., Schense, J.C., Kohler, T., Müller, R., Hubbell, J.A., 2003. Repair of bone defects using synthetic mimetics of collagenous extracellular matrices. Nat. Biotechnol. 21, 513–518. https://doi.org/10.1038/nbt818.
Maddalozzo, G.F., Turner, R.T., Edwards, C.H.T., Howe, K.S., Widrick, J.J., Rosen, C.J., Iwaniec, U.T., 2009. Alcohol alters whole body composition, inhibits bone formation, and increases bone marrow adiposity in rats. Osteoporos. Int. 20, 1529–1538. https://doi.org/10.1007/s00198-009-0836-y.
Marins, L.V., Cestari, T.M., Sottovia, A.D., Granjeiro, J.M., Taga, R., 2004. Radiographic and histological study of perennial bone defect repair in rat calvaria after treatment with blocks of porous bovine organic graft material. J. Appl. Oral Sci. 12, 62–69 https://doi.org/S1678-77572004000100012[pii].
Marsell, R., Einhorn, T.A., 2010. Emerging bone healing therapies. J. Orthop. Trauma 24, 4–8. https://doi.org/10.1097/BOT.0b013e3181ca3fab.
Más, B.A., Freire, D.C., de, L., Cattani, S.M., de, M., Motta, Barbo, A.C., Peris, M.L., Duek, E.A., de, R., 2016. Biological evaluation of PLDLA polymer synthesized as construct on bone tissue engineering application. Mater. Res. 19, 300–307. https://doi.org/10.1590/1980-5373-MR-2015-0559.
Maurel, D.B., Boisseau, N., Ingrand, I., Dolleans, E., Benhamou, C.L., Jaffre, C., 2011. Combined effects of chronic alcohol consumption and physical activity on bone health: study in a rat model. Eur. J. Appl. Physiol. 111, 2931–2940. https://doi.org/10.1007/s00421-011-1916-1.
Maurel, D.B., Boisseau, N., Benhamou, C.L., Jaffre, C., 2012. Alcohol and bone: review of dose effects and mechanisms. Osteoporos. Int. 23, 1–16. https://doi.org/10.1007/s00198-011-1787-7.
Messingham, K.A.N., Faunce, D.E., Kovacs, E.J., 2002. Alcohol, injury, and cellular immunity. Alcohol 28, 137–149. https://doi.org/10.1016/S0741-8329(02)00278-1.
Napolitano, L.M., Koruda, M.J., Zimmerman, K., McCowan, K., Chang, J.J., Meyer, A.A., 1995. Chronic ethanol intake and burn injury - evidence for synergistic alteration in nut and immune integrity. J. Trauma-Injury Infect. Crit. Care 38, 198–207. https://doi.org/10.1097/00005373-199502000-00008.
Neagu, T.P., Ţigliş, M., Cocoloş, I., Jecan, C.R., 2016. The relationship between periosteum and fracture healing. Rom. J. Morphol. Embryol. 57, 1215–1220.
Newman, L., Curran, M., GL, B., 1986. Effects of chronic alcohol intake on anesthetic responses to diazepam and thiopental in rats. Anesthesiology.
Nkenke, E., Neukam, F., 2014. Autogenous bone harvesting and grafting in advanced jaw resorption: morbidity, resorption and implant survival. Eur J Oral Implant 7, 203–2017. https://doi.org/10.1016/S0377-1237(17)30293-9.
Pilipchuk, S.P., Plonka, A.B., Monje, A., Taut, A.D., Kang, B., Giannobile, W.V., Arbor, A., Medicine, O., 2015. Tissue Engineering for Bone Regeneration and Osseointegration in the Oral Cavity. Dent. Mater. 31, 317–338. https://doi.org/10.1016/j.dental.2015.01.006.Tissue.
Pomini, K.T., Andreo, J.C., De Rodrigues, A.C., De Gonçalves, J.B.O., Daré, L.R., German, I.J.S., Rosa, G.M., Buchaim, R.L., 2014. Effect of low-intensity pulsed ultrasound on bone regeneration biochemical and radiologic analyses. J. Ultrasound Med. 33, 713–717. https://doi.org/10.7863/ultra.33.4.713.
Qiu, Q., Mendenhall, H.V., Garlick, D.S., Connor, J., 2007. Evaluation of bone regeneration at critical-sized calvarial defect by DBM/AM composite. J. Biomed. Mater. Res. B Appl. Biomater. 81, 516–523.
Ramalingam, S., Al-Rasheed, A., ArRejaie, A., Nooh, N., Al-Kindi, M., Al-Hezaimi, K., 2016. Guided bone regeneration in standardized calvarial defects using beta-tricalcium phosphate and collagen membrane: a real-time in vivo micro-computed tomographic experiment in rats. Odontology 104, 199–210. https://doi.org/10.1007/s10266-015-0211-8.
Rocha, C.A., Cestari, T.M., Vidotti, H.A., De Assis, G.F., Garlet, G.P., Taga, R., 2014. Sintered anorganic bone graft increases autocrine expression of VEGF, MMP-2 and MMP-9 during repair of critical-size bone defects. J. Mol. Histol. 45, 447–461. https://doi.org/10.1007/s10735-014-9565-4.
Sakkas, A., Wilde, F., Heufelder, M., Winter, K., Schramm, A., 2017. Autogenous bone grafts in oral implantology—is it still a “gold standard”? A consecutive review of 279 patients with 456 clinical procedures. Int. J. Implant Dent. 3 (23). https://doi.org/10.1186/s40729-017-0084-4.
Santana, W.M., de, S., de Ferreira, D.N., Duarte Maria, V., Rodrigues, W., 2016. Simvastatin and biphasic calcium phosphate affects bone formation in critical-sized rat calvarial defects. Acta Cir. Bras. 31, 300–307. https://doi.org/10.1590/S0102-865020160050000002.
Schmidlin, P.R., Nicholls, F., Kruse, A., Zwahlen, R.A., Weber, F.E., 2013. Evaluation of moldable, in situ hardening calcium phosphate bone graft substitutes. Clin. Oral Implants Res. 24, 149–157. https://doi.org/10.1111/j.1600-0501.2011.02315.x.
Soares, E.V., Fávaro, W.J., Cagnon, V.H.A., Bertran, C.A., Camilli, J.A., 2010. Effects of alcohol and nicotine on the mechanical resistance of bone and bone neoformation around hydroxyapatite implants. J. Bone Miner. Metab. 28, 101–107. https://doi.org/10.1007/s00774-009-0115-1.
Spicer, P.P., Kretlow, J.D., Young, S., Jansen, Ja, Kasper, F.K., Mikos, A.G., Kurtis, F., Mikos, A.G., 2013. Evaluation of bone regeneration using the rat critical size calvarial defect. NIH Public Access 7, 1918–1929. https://doi.org/10.1038/nprot.2012.113.Evaluation.
Sreenathan, R.N., Singh, S., Padmanabhan, R., 1984. Effect of acetaldehyde on skeletogenesis in rats. Drug Alcohol Depend. 14, 165–174. https://doi.org/10.1016/0376-8716(84)90041-3.
Taniyama, K., Shirakata, Y., Yoshimoto, T., Takeuchi, N., Yoshihara, Y., Noguchi, K., 2013. Bone formation using β-tricalcium phosphate/carboxymethyl-chitin composite scaffold in rat calvarial defects. Oral Surg. Oral Med. Oral Pathol. Oral Radiol. 116, e450–e456. https://doi.org/10.1016/j.oooo.2012.02.033.
Tonnesen, H., 2003. Alcohol abuse and postoperative morbidity. Dan. Med. Bull. 50, 139–160.
Trevisiol, C.H., Turner, R.T., Pfaff, J.E., Hunter, J.C., Menagh, P.J., Hardin, K., Ho, E., Iwaniec, U.T., 2007. Impaired osteoinduction in a rat model for chronic alcohol abuse. Bone 41, 175–180. https://doi.org/10.1016/j.bone.2007.04.189.
Verhaeghe, N., Lievens, D., Annemans, L., Vander Laenen, F., Putman, K., 2017. The health-related social costs of alcohol in Belgium. BMC Public Health 17, 1–11. https://doi.org/10.1186/s12889-017-4974-4.
Verna, C., Bosch, C., Dalstra, M., Wikesjö, U.M.E., Trombelli, L., 2002. Healing patterns in calvarial bone defects following guided bone regeneration in rats: a micro-CT scan analysis. J. Clin. Periodontol. 29, 865–870. https://doi.org/10.1034/j.1600-051X.2002.290912.x.
Winn, S.R., Schmitt, J.M., Buck, D., Hu, Y., Grainger, D., Hollinger, J.O., 1999. Tissue-engineered bone biomimetic to regenerate calvarial critical- sized defects in athymic rats. J. Biomed. Mater. Res. 45, 414–421. https://doi.org/10.1002/(SICI)1097-4636(19990615)45:4<414::AID-JBM17>3.0.CO;2-Z.
Yang, C., Unursaikhan, O., Lee, J.S., Jung, U.W., Kim, C.S., Choi, S.H., 2014. Osteoconductivity and biodegradation of synthetic bone substitutes with different tricalcium phosphate contents in rabbits. J. Biomed. Mater. Res. - B Appl. Biomater. 102, 80–88. https://doi.org/10.1002/jbm.b.32984.
Zhu, H., Yang, F., Tang, B., Li, X.M., Chu, Y.N., Liu, Y.L., Wang, S.G., Wu, D.C., Zhang, Y., 2015. Mesenchymal stem cells attenuated PLGA-induced inflammatory responses by inhibiting host DC maturation and function. Biomaterials 53, 688–698. https://doi.org/10.1016/j.biomaterials.2015.03.005.
Zong, C., Xue, D., Yuan, W., Wang, W., Shen, D., Tong, X., Shi, D., Liu, L., Zheng, Q., Gao, C., Wang, J., 2010. Reconstruction of rat calvarial defects with human mesenchymal stem cells and osteoblast-like cells in poly-lactic-co-glycolic acid scaffolds. Eur. Cells Mater. 20, 109–120. https://doi.org/10.22203/eCM.v020a10.